Since January 2020 Elsevier has created a COVID-19 resource centre with free information in English and Mandarin on the novel coronavirus COVID-19. The COVID-19 resource centre is hosted on Elsevier Connect, the company's public news and information website.

Biosafety and Health 4 (2022) 186–192

Contents lists available at ScienceDirect

Biosafety and Health

journal homepage: www.elsevier.com/locate/bsheal

Screening for inhibitors against SARS-CoV-2 and its variants

Weijing Yuan [a,1], Xiaojing Dong [a,1], Lan Chen [a,1], Xiaobo Lei [a], Zhuo Zhou [b,c,*], Li Guo [a,*], Jianwei Wang [a,2]

[a] Institute of Pathogenic Biology, Peking Union Medical College, Chinese Academy of Medical Sciences, Beijing 100730, China
[b] School of Life Science, Peking University, Beijing 100871, China
[c] Biomedical Pioneering Innovation Center, Peking University, Beijing 100871, China

ARTICLE INFO

Article history:
Received 27 April 2022
Revised 4 May 2022
Accepted 5 May 2022
Available online 7 May 2022

Keywords:
SARS-CoV-2
Delta variant
Omicron variant
Trifluoperazine 2HCl
Thioridazine HCl
Antiviral therapy

ABSTRACT

Severe acute respiratory syndrome coronavirus 2 (SARS-CoV-2) continues to evolve, generating new variants that pose a threat to global health; therefore, it is imperative to obtain safe and broad-spectrum antivirals against SARS-CoV-2 and its variants. To this end, we screened compounds for their ability to inhibit viral entry, which is a critical step in virus infection. Twenty compounds that have been previously reported to inhibit SARS-CoV-2 replication were tested by using pseudoviruses containing the spike protein from the original strain (SARS-CoV-2-WH01). The cytotoxicity of these compounds was determined. Furthermore, we identified six compounds with strong antagonistic activity against the WH01 pseudovirus, and low cytotoxicity was identified. These compounds were then evaluated for their efficacy against pseudoviruses expressing the spike protein from B.1.617.2 (Delta) and B.1.1.529 (Omicron), the two most prevalent circulating strains. These assays demonstrated that two phenothiazine compounds, trifluoperazine 2HCl and thioridazine HCl, inhibit the infection of Delta and Omicron pseudoviruses. Finally, we discovered that these two compounds were highly effective against authentic SARS-CoV-2 viruses, including the WH01, Delta, and Omicron strains. Our study identified potential broad-spectrum SARS-CoV-2 inhibitors and provided insights into the development of novel therapeutics.

1. Introduction

Coronavirus disease 2019 (COVID-19) is caused by severe acute respiratory syndrome coronavirus 2 (SARS-CoV-2) and has spread rapidly throughout the globe. According to the most recent World Health Organization (WHO) report published on April 29, 2022, there have been 510.2 million confirmed cases of COVID-19, with 6.23 million deaths [1]. As the pandemic progressed, SARS-CoV-2 evolved into mutant strains such as B.1.617.2 (Delta) and B.1.1.529 (Omicron). The emergence of these variants complicates vaccine prevention and control, and the process of developing broad-spectrum vaccines or drugs is lengthy and unpredictable. Therefore, it is beneficial to search for approved compounds with broad-spectrum antiviral activity against SARS-CoV-2. Many drugs have been reported to be effective at inhibiting SARS-CoV-2 infection, including Remdesivir, which inhibits virus replication *in vitro* [2], and Dexamethasone, which demonstrated remarkable therapeutic effects in critically ill COVID-19 patients [3]. However, both have only a marginal effect on mild COVID-19 patients [4]. Other potential drugs, such as chloroquine and hydroxychloroquine [5,6], are not widely applicable due to their systemic toxicity and associated risk of use [7,8]. Recently, the U.S. Food and Drug Administration (FDA) has approved the emergency use of the unapproved product Paxlovid for the treatment of mild-to-moderate COVID-19 [9]; however, the efficacy of this drug needs to be clinically validated. Collectively, repurposing approved drugs for COVID-19 is required to contain the pandemic in a timely manner.

Antivirals can target multiple stages of the SARS-CoV-2 replication cycle. For instance, efforts have been made to identify drugs that specifically target the main protease (M^{pro}), the papain-like protease (PL^{pro}), or the RNA-dependent RNA polymerase (RdRp), all of which are required for viral genome replication and transcription [10–14]. Furthermore, in theory, viral entry is an attractive target step because it prevents viral entry and, as such, appears to be the most efficient way to combat virus infection and spread. Thus, it is worthwhile to establish a strategy for screening drugs that inhibit SARS-CoV-2 entry.

Previously, we conducted high-throughput screening of approximately 1,700 U.S. FDA-approved compounds to identify agents cap-

* Corresponding authors: Institute of Pathogenic Biology, Peking Union Medical College, Chinese Academy of Medical Sciences, Beijing 100730, China (Z. Zhou, L. Guo).
E-mail addresses: zhouzhuo@gmail.com (Z. Zhou), gnyny0803@163.com (L. Guo).

[1] These authors contributed equally to this work.

[2] Given his role as Executive Editor-in-Chief, Jianwei Wang had no involvement in the peer-review of this article and had no access to information regarding its peer-reivew. Full responsibility for the editorial process for this article was delegated to the Editor Guizhen Wu.

https://doi.org/10.1016/j.bsheal.2022.05.002

HIGHLIGHTS

Scientific question

This study aims to determine which FDA-approved compound(s) can be repurposed as a broad-spectrum antiviral drug(s) against SARS-CoV-2 and variants.

Evidence before this study

Drug repurposing is a widely used strategy for identifying new uses for approved or investigational drugs that are not covered by the approved or investigational indication. Numerous currently available drugs, including Remdesivir, Dexamethasone, and hydroxychloroquine, have been evaluated for their efficacy in treating COVID-19 to combat the pandemic. However, the applicability of these drugs is limited by efficacy and safety concerns. As the pandemic progresses, the SARS-CoV-2 virus evolves globally, necessitating the development of broad-spectrum antiviral drugs via drug repurposing strategies.

New findings

By using pseudotyped and authentic SARS-CoV-2 strains, this study determined that the phenothiazine compounds trifluoperazine 2HCl and thioridazine HCl could potently inhibit SARS-CoV-2 entry with low cytotoxicity. Additionally, these two compounds exhibit broad antiviral activity against the SARS-CoV-2-WH01, B.1.617.2 (Delta), and B.1.1.529 (Omicron) virus strains.

Significance of the study

Trifluoperazine 2HCl and thioridazine HCl were initially identified as phenothiazine compounds capable of inhibiting the entry of SARS-CoV-2 and its circulating variants with minimal cytotoxicity. Phenothiazine compounds may be a promising drug lead for the development of effective and broad-spectrum COVID-19 cures.

able of inhibiting SARS-CoV-2 replication and successfully identified 20 anti-SARS-CoV-2 compounds [15]. However, it is unknown whether these drugs can inhibit viral entry or possess broad antiviral activity against SARS-CoV-2 variants. Thus, we used pseudovirus-based assays to determine whether these compounds inhibit viral entry. We then investigated the effect of the compound hits on pseudotyped and authentic SARS-CoV-2 strains, including the original strain WH01, as well as Delta and Omicron variants.

2. Materials and methods

In this study, the Polybrene and Cell Counting Kit (CCK-8) was purchased from Yeasen Biotechnology Co., Ltd. (40203ES80, Shanghai, China). Luciferase® Assay System was purchased from Promega (E1500, Wisconsin, USA). Direct-zol™ RNA MiniPrep was purchased from ZYMO Research (R2052, California, USA). TRIzol™ LS Reagent was purchased from Thermo Fisher Scientific (10296028, Massachusetts, USA).

2.1. Cell lines

HEK293T cells used were purchased from American Type Culture Collection. HEK293T-ACE2 cell lines were established and stored in our lab. Cells were cultured in Dulbecco's Modified Eagle Medium (DMEM, Gibco, USA) containing 10% Fetal Bovine Serum (FBS, HyClone, USA) at 37 ℃ and 5% CO_2.

2.2. SARS-CoV-2 infection

SARS-CoV-2 strains, including WH01 (IPBCAMS-WH-01/2019), B.1.617.2 (Delta), and B.1.1.529 (Omicron) were propagated in Vero cells and stored in a BSL-3 laboratory. All infection experiments were performed in a BSL-3 environment.

2.3. Pseudovirus production

HEK293T cells were plated at a density of 7×10^6 cells per 10-cm cell culture dish. Following 12 h of culture, 5 μg of pCAGGS-WH01-S/Omicron-S or pLV-Delta-S, 3 μg of plenti-Luc, and 4 μg of psPAX2 plasmids were combined, and PEI transfected. After 6–8 h transfection, the supernatant was replaced with DMEM containing 10% FBS. Then, 48 h after transfection, the supernatant was collected and centrifuged at 4 ° C for 10 min at 3,000g. The supernatant containing pseudovirus was collected and stored at −80 ˚C.

2.4. Cytotoxicity of compounds was detected by CCK-8 assay

HEK293T-ACE2 cells were seeded in 96 well plates at 4×10^4 cells per well. After 12 h, the culture supernatant was discarded. The compound solution was diluted with DMEM containing 10% FBS (final concentration: 2 μM, 5 μM). Dimethyl sulfoxide (DMSO) was used as the control. Each compound was tested in three separate wells at three different concentrations, and the cells were incubated for 24 h at 37 ˚C with 5% CO_2. Next, 10 μL of CCK-8 solution was added to each well and culture for an additional 1–4 h. SpectraMax M5 was used to detect the OD value at 450 nm, and the cell viability was calculated and plotted according to the formula:

$$\text{Cell Viability (\%)} = [\text{dose-blank (no cells)}]/[\text{undosed (DMSO)} - \text{blank (no cells)}]$$

2.5. The measurement of pseudovirus infectivity by the Luciferase Assay System

HEK293T-ACE2 cells were seeded in 96 well plates at 4×10^4 cells per well. The supernatant was discarded after 12 h of culture, and the compound solution was diluted with DMEM containing 10% FBS (final concentration is 2 μM, 5 μM). Three multiple wells of each compound were set up at each concentration and treated for 1 h. Polybrene was added to the pseudovirus solution at a final concentration of 8 μg/mL, and each well was filled with 100 μL pseudovirus solution. After 12 h of infection, the supernatants were replaced with DMEM (containing 10% FBS) containing the compound to be quantified at the corresponding concentration. The infection was continued for 48 h. Then, cells were lysed in 50 μL 1 × Passive Lysis Buffer, and luciferase assays using the Luciferase® Assay System (Promega, E1500, Wisconsin, USA) were performed according to the manufacturer's instructions. Luciferase activity was normalized and represented as a percentage of the value determined in the DSMO control.

2.6. Western blot analysis

HEK293T-ACE2 cells were pretreated with S-Ruxolitinib (final concentration is 4 μM) for 1 h and infected with SeV for 24 h. Cells were then lysed in RIPA (Radio-Immunoprecipitation) buffer. The protein samples were separated on SDS-PAGE gels, transferred onto nitrocellulose membranes, and immunoblotted with indicated primary and secondary antibodies. The expression levels of indicated proteins were detected by the Odyssey Infrared Imaging System and quantified by ImageStudio (Software from LI-COR Biosciences), Western blots underwent semi-quantitative analysis of gray intensity. The ratio of pSTAT1/STAT1 was normalized to the DMSO-treated control.

2.7. Dose-response curve and IC_{50} determination

HEK293T-ACE2 cells were seeded at a density of 4×10^4 cells per well in 96 well plates. After 12 h, the supernatant was discarded, and cells were pre-treated for 1 h with compound at concentrations of 0.013, 0.041, 0.123, 0.370, 1.111, 3.333, 10, and 30 μM for 1 h, followed by infection with SARS-CoV-2 (WH01/Delta/Omicron) at an MOI of 0.1 for 24 h. The supernatant from each well was then added to TRIzol LS reagent, and the supernatant was used to extract viral RNAs using Direct-zol™ RNA MiniPrep. The amount of viral RNA was determined using qRT-PCR to detect SARS-CoV-2 nucleocapsid RNA, and the virus copies were calculated using standard curves. The standard curves were plotted according to ten-fold serial diluted reference standards (1.04×10^9 to 1.04×10^4 copies). GraphPad Prism 8 was used to calculate the half-maximal inhibitory concentration (IC_{50}).

2.8. Immunofluorescence

In confocal dishes, HEK293T-ACE2 cells were infected for 24 h with SARS-CoV-2 (WH01/ Delta/Omicron) at an MOI of 0.1 in BSL-3. Infected cells were fixed for 30 min at room temperature in 4% Paraformaldehyde and then soaked overnight in 4% paraformaldehyde at 4 ˚C to further inactivate the virus. The cells were then permeabilized for 10 min with a 0.5% Triton X-100 solution. The confocal dishes were filled with 5% Bovine Serum Albumin (BSA) in PBS and sealed overnight at 4 ˚C. The following day, the supernatant was discarded, and a diluted antibody against SARS-CoV-2 nucleocapsid (N) protein was added. Subsequently, cells were incubated overnight at 4 ˚C. Confocal dishes were washed three times (10 min each time) with 1% PBST (PBS + 1% Tween 20), then incubated for 1 h at room temperature with cross-adsorbed secondary antibodies. Nucleocapsids were stained with an Alexa Fluor 488. Nuclei were stained with 4',6-diamidino-2-phenylindole (DAPI). The Zeiss LSM 800 Confocal Laser Scanning Microscope was used to acquire the images.

2.9. Statistical analysis

GraphPad Prism 8 was used to perform the two-tailed Student's *t*-test to determine the significance of the difference between two-group comparisons. $^*P < 0.05$, $^{**}P < 0.01$, $^{***}P < 0.001$, $^{****}P < 0.001$; NS, not significant.

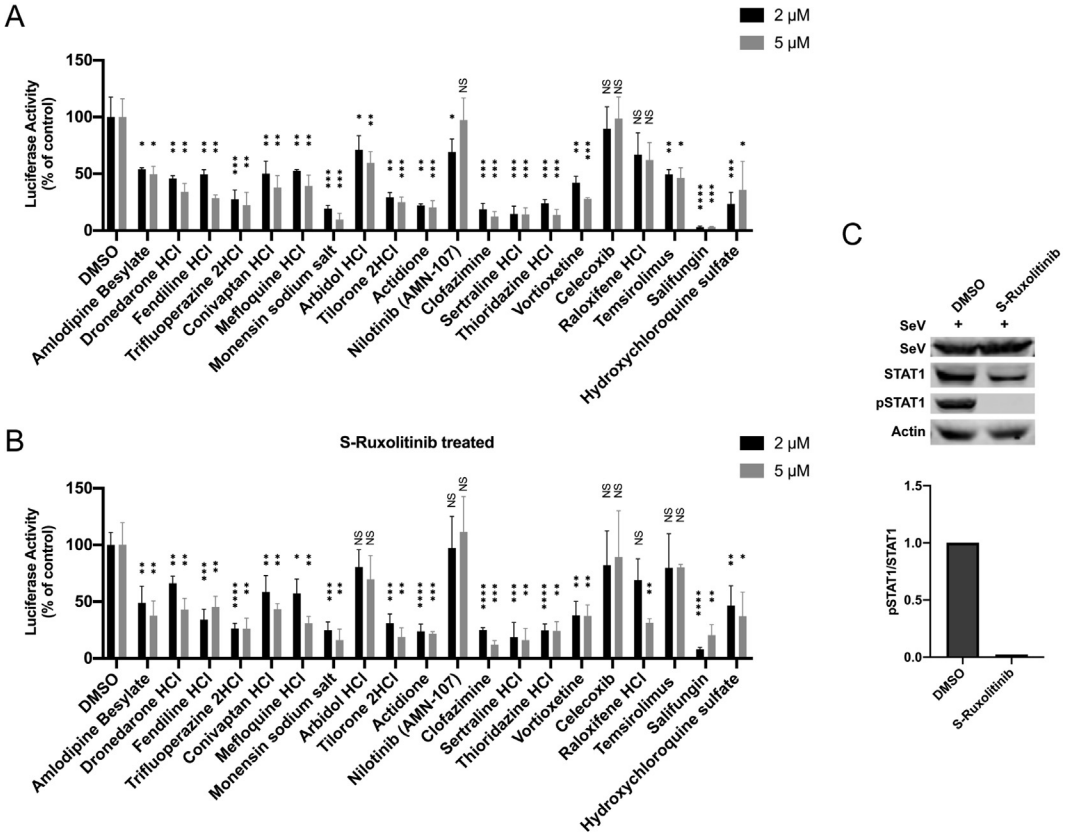

Fig. 1. Evaluation of the effectiveness of 20 compounds on SARS-CoV-2-WH01 pseudovirus infection. A) SARS-CoV-2-WH01 pseudovirus infection assay. HEK293T-ACE2 cells were pretreated with indicated 20 compounds at two doses (2 μM, 5 μM) for 1 h. Then, cells were infected with SARS-CoV-2-WH01 pseudovirus. After 48 h, cells were lysed and the luciferase activity was measured. Luciferase activity was normalized and represented as a percentage of the value determined in the Dimethyl sulfoxide (DMSO) control. The experiments were performed in triplicate and repeated three times. Error bars represent ± SD. $^*P < 0.05$, $^{**}P < 0.01$, $^{***}P < 0.001$, $^{****}P < 0.0001$, two-tailed Student's *t*-test. B) SARS-CoV-2-WH01 pseudovirus infection assay under STAT1 inhibition. HEK293T-ACE2 cells were pretreated with S-Ruxolitinib (4 μM) and 20 compounds (2 μM, 5 μM) for 1 h, and were then infected with SARS-CoV-2-WH01 pseudovirus for 48 h. Cells were lysed and the luciferase activity was measured. The experiments were performed in triplicate and repeated three times. Error bars represent ± SD. $^*P < 0.05$, $^{**}P < 0.01$, $^{***}P < 0.001$, $^{****}P < 0.0001$, two-tailed Student's *t*-test. C) S-Ruxolitinib effectively inhibits STAT1 phosphorylation. HEK293T-ACE2 cells were pretreated with S-Ruxolitinib (4 μM) for 1 h and infected with SeV for 24 h. The levels of phosphorylated STAT1 (pSTAT1) and total STAT1 were detected by Western blot with indicated antibodies (Upper). The experiments were performed twice, and one representative is shown. Western blots underwent semi-quantitative analysis of gray intensity, and the ratio of pSTAT1/STAT1 was normalized to DMSO-treated controls. The mean values of two replicates were shown (Lower).

3. Results

3.1. Identification of compounds that inhibit SARS-CoV-2-WH01 pseudovirus infection

In order to identify agents that inhibit SARS-CoV-2 entry, we used pseudoviruses to test 20 previously reported compounds. HEK293T-ACE2 cells were incubated for 1 h with DMSO as a control or the indicated compounds at two concentrations (2 μM, 5 μM). The cells were then infected with the pseudovirus harboring spike protein from the original strain (SARS-CoV-2-WH01) and a luciferase reporter gene. After 48 h, luciferase assays were used to determine pseudovirus infectivity. Trifluoperazine 2HCl, monensin sodium salt, tilorone 2HCl, actidione, clofazimine, sertraline HCl, thioridazine HCl, vortioxetine, and salifungin significantly inhibited SARS-CoV-2-WH01 pseudovirus infection at both doses, by more than 50%, suggesting that these nine drugs can impede the cellular entry of SARS-CoV-2.

As chemical drugs may indirectly inhibit viral entry by stimulating the host's antiviral immune response, it is important to determine whether these components directly or indirectly inhibit viral entry via modulation of cytokine production. To address this, we examined the efficacy of 20 compounds on SARS-CoV-2-WH01 pseudovirus entry when the JAK-STAT pathway was inhibited, a critical pathway that regulates the expression of multiple antiviral cytokines, including type I, II, and III interferons (IFNs) [16]. S-Ruxolitinib, a highly selective and potent inhibitor of JAK 1/2, was chosen to inhibit JAK-STAT activation. We found that nine preliminarily identified compounds showed comparable inhibitory effects on WH01 pseudovirus infection in the absence or presence of S-Ruxolitinib (Fig. 1A and 1B), indicating that these compounds inhibit viral entry independently of antiviral cytokines. Furthermore, the efficacy of S-Ruxolitinib in inhibiting JAK-STAT signaling was demonstrated by decreased STAT1 phosphorylation induced by Sendai Virus infection (Fig. 1C).

3.2. Evaluation of cytotoxicity of the compounds

We further examined the cytotoxicity of the compounds. Cell Counting Kit-8 (CCK-8) was used to determine the viability of cells following treatment with 20 drugs at two different concentrations (2 μM, 5 μM) (Fig. 2). This demonstrated that actidione, temsirolimus, salifungin,

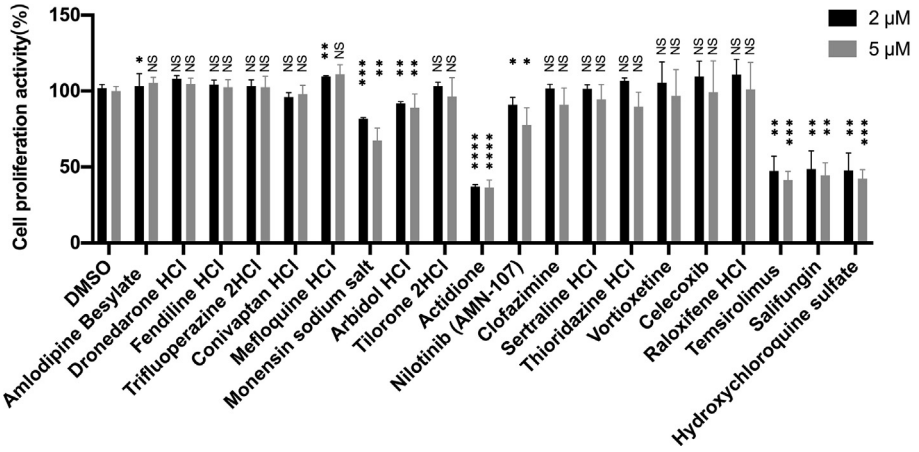

Fig. 2. Cytotoxicity assay of 20 compounds to HEK293T-ACE2. The CCK-8 kit was used to determine the cytotoxicity of 20 compounds at two concentrations (2 μM, 5 μM). Cell viability was calculated and plotted using the formula. The experiments were performed twice, and one representative is shown. Error bars represent ± SD. $^{*}P < 0.05$, $^{**}P < 0.01$, $^{***}P < 0.001$, $^{****}P < 0.0001$, two-tailed Student's *t*-test.

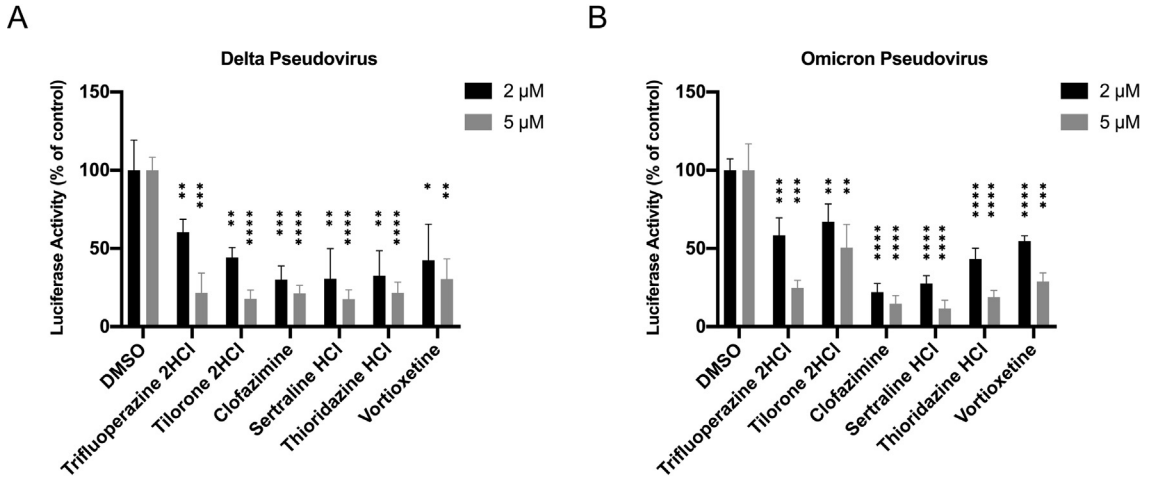

Fig. 3. Antiviral activity of six compounds against the SARS-CoV-2-Delta/Omicron pseudovirus. A and B) HEK293T-ACE2 cells were pretreated with 6 indicated compounds at two doses (2 μM, 5 μM) for 1 h. Then, cells were infected with Delta A) or Omicron B) pseudovirus. After 48 h, cells were lysed and the luciferase activity was measured. Luciferase activity was normalized and represented as a percentage of the value determined in the Dimethyl sulfoxide (DMSO) control. The experiments were performed in triplicate and repeated three times. Error bars represent ± SD. $^{*}P < 0.05$, $^{**}P < 0.01$, $^{***}P < 0.001$, $^{****}P < 0.0001$, two-tailed Student's *t*-test.

and hydroxychloroquine sulfate treatment significantly decreased cell viability. Monensin sodium salt also showed cytotoxicity, albeit to a lesser extent. Other drugs showed low cytotoxicity, with the relative cell viability remaining above 90%. Considering the antiviral effect and cytotoxicity of the compounds, we selected trifluoperazine 2HCl, tiloronе 2HCl, vortioxetine, clofazimine, sertraline HCl, and thioridazine HCl for further analysis with Delta and Omicron variants.

3.3. Evaluation of the efficacy of six candidate compounds on Delta and Omicron pseudovirus infection

Six SARS-CoV-2-WH01 entry inhibitors were then tested for their effect on other circulating strains. We developed Delta and Omicron pseudoviruses that contain both the spike protein and the luciferase reporter gene. Again, HEK293T-ACE2 cells were pre-treated with six compounds at two different concentrations (2 μM, 5 μM) prior to infection with the pseudovirus. Subsequently, luciferase assays were used to determine the pseudovirus infectivity (Fig. 3). We discovered that 5 μM of trifluoperazine 2HCl, vortioxetine, clofazimine, sertraline HCl, and thioridazine HCl effectively inhibited Delta and Omicron pseudovirus infection by more than 60%, implying that these compounds exhibit broad-spectrum activity. Notably, the effect of two phenothiazine drugs, trifluoperazine 2HCl and thioridazine HCl, on SARS-CoV-2 entry, was previously unknown.

3.4. Effects of trifluoperazine 2HCl and thioridazine HCl on authentic SARS-CoV-2 viruses

Then, we investigated whether the phenothiazine drugs trifluoperazine 2HCl and thioridazine HCl could inhibit infection with authentic

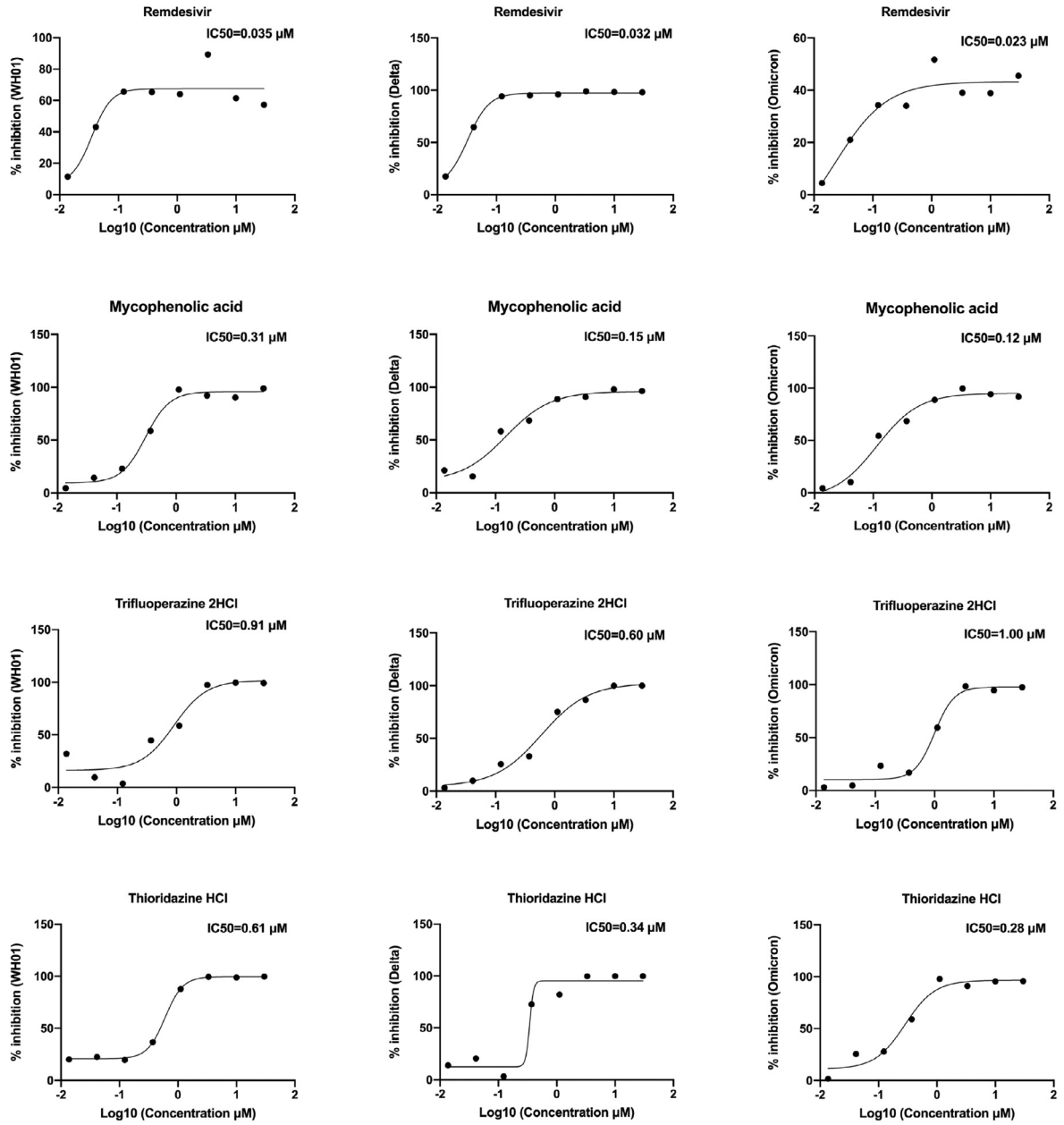

Fig. 4. Determination of effective concentrations of the compounds against authentic SARS-CoV-2 infection. HEK293T-ACE2 cells were pretreated with serially diluted compounds (0.014, 0.041, 0.123, 0.370, 1.111, 3.333, 10.000, and 30.000 μM) at 37 °C for 1 h and then infected with 0.1 MOI of authentic SARS-CoV-2 strains including WH01, Delta, and Omicron for 24 h. qRT-PCR was used to determine the viral load in the cell supernatant. The figure's Y-axis depicts the percentage inhibition of virus replication.

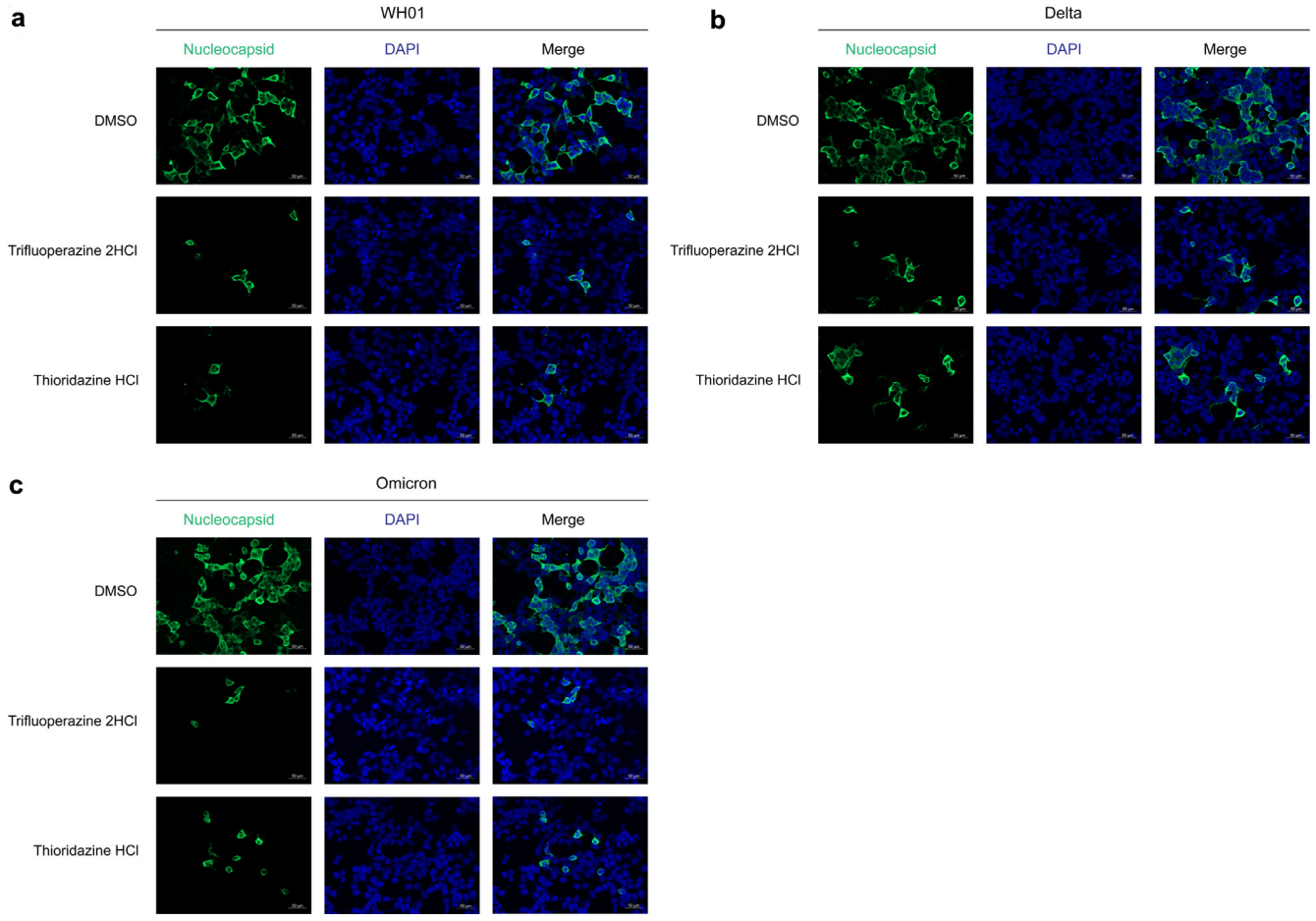

Fig. 5. Effect of compounds on authentic SARS-CoV-2 infection. HEK293T-ACE2 cells were pre-treated with 5 μM indicated compounds at 37 °C for 1 h and then infected with 0.1 MOI of authentic SARS-CoV-2 strains including A) WH01, B) Delta, and C) Omicron for 24 h. Infected cells were fixed and stained with an anti-nucleocapsid antibody (green). Nuclei were stained with 4',6-diamidino-2-phenylindole (DAPI) (blue). Dimethyl sulfoxide (DMSO) was used as the control. Cells were then subjected to confocal microscopy analysis. Scale bars, 50 μm.

SARS-CoV-2 viruses. To accomplish this, we treated HEK293T-ACE2 cells with serially diluted concentrations of the two compounds. Afterward, we infected cells in the BSL-3 laboratory with authentic SARS-CoV-2-WH01 virus, as well as Delta and Omicron variants, and detected virus load using qRT-PCR. Remdesivir and mycophenolic acid were used as controls because they had been shown to effectively inhibit SARS-CoV-2 infection [17]. The dose–response curves were then plotted, and the half inhibitory concentration (IC_{50}) was determined to determine the effective concentrations. Both compounds inhibited replication of all authentic SARS-CoV-2 viruses at submicromolar concentrations (Fig. 4), indicating their potential use as broad-spectrum antiviral drug candidates or leads.

Then, we used an immunofluorescence assay to determine the effect of trifluoperazine 2HCl and thioridazine HCl. We observed that trifluoperazine 2HCl and thioridazine HCl significantly inhibited the expression of SARS-CoV-2 nucleocapsid protein in cells infected with WH01, Delta, and Omicron viruses when compared to DMSO treatment (Fig. 5), confirming their broad-spectrum antiviral activity.

4. Conclusion and discussion

In this study, we used 20 compounds previously reported to be effective at inhibiting SARS-CoV-2 replication [15] as screening objects. The effects of the drug on viral entry, a pivotal step in the virus's establishment of virus infection, were determined using pseudovirus assays. Of the 20 drugs tested, 5 (trifluoperazine 2HCl, vortioxetine, clofazimine, sertraline HCl, and thioridazine HCl) were effective in inhibiting WH01, Delta, and Omicron pseudovirus infection. Among them, the activity of trifluoperazine 2HCl and thioridazine HCl on viral entry was reported for the first time, while the other three drugs, vortioxetine, clofazimine, and sertraline HCl, were previously associated with the efficacy of inhibiting SARS-CoV-2 entry. Vortioxetine is a well-tolerated and safe antidepressant [18] frequently used to treat adults with severe depressive disorder.

Additionally, vortioxetine exhibited effective inhibition of SARS-CoV-2 entry, but the underlying mechanism is unknown [19]. Clofazimine was initially discovered as a tuberculosis treatment and later as a leprosy treatment [20]. Clofazimine is a low-cost, safe, and well-tolerated medication [21]. The drug was found to inhibit SARS-CoV-2 replication in various ways, including by inhibiting Spike-dependent viral entry and replication [22,23]. Sertraline HCl, an antidepressant, has also been shown to inhibit SARS-CoV-2 and pp-VSV-SARS-CoV-2 pseudovirus infection [24]. Another report indicates that it inhibits SARS-CoV-2 replication [25].

To our knowledge, the phenothiazine compounds trifluoperazine 2HCl and thioridazine HCl were the first to be identified as low-cytotoxicity inhibitors of SARS-CoV-2 entry. Phenothiazine compounds are commonly used to treat acute and chronic psychosis [26,27] and inhibit dopamine D2 receptors and α2-Adrenergic receptors (α2). In 1986, trifluoperazine was found to promote the conformation of Sendai Virus fusion protein F, thereby inhibiting virus-red blood cell fusion and hemolysis [28]. Coincidentally, trifluoperazine has been shown to inhibit the membrane fusion of the Mouse Leukemia Virus and thus effectively reduce viral infection [29]. As trifluop-

erazine inhibits the entry of pseudotyped or authentic WH01, Delta, and Omicron viruses, we hypothesize that trifluoperazine functions by modulating the conformational change of the SARS-CoV-2 spike, resulting in its transition from fusion to non-fusion state.

The SARS-CoV-2 S pseudovirus is based on the lentiviral vector. It carries virus spikes but does not replicate. In comparison to authentic SARS-CoV-2, which must be operated in a BSL-3 environment, the use of pseudovirus significantly reduces the difficulty and complexity of experimental operations and significantly accelerates drug screening. On the other hand, pseudovirus-based screens may miss drug hits targeting non-entry steps. Thus, combining the pseudovirus and authentic virus assay will generate optimal antiviral screening results.

The emergence and spread of SARS-CoV-2 variants Delta and Omicron have sparked global concern. At sub-micromolar concentrations, the newly identified FDA-approved phenothiazine compounds trifluoperazine 2HCl and thioridazine HCl can inhibit the replication of these variants. Additionally, these two drugs have low cytotoxicity. Thus, we hypothesized that phenothiazine compounds could be a promising drug lead for developing potent and broad-spectrum cures for COVID-19.

Acknowledgements

This work was supported by grants from National Key R&D Program of China (2020YFA0707600 to Z.Z. and X.L.), the National Natural Science Foundation of China (81930063 and 81971948 to J.W. and X.L.), and Chinese Academy of Medical Science (CAMS) Innovation Fund for Medical Sciences (2021-I2M-1-038 to J.W.)

Conflict of interest statement

The authors declare that there are no conflicts of interest.

Author contributions

Weijing Yuan: Investigation, Validation, Formal Analysis, Data Curation, Visualization, Writing - Original Draft. **Xiaojing Dong:** Investigation, Validation. **Lan Chen:** Investigation, Validation. **Xiaobo Lei:** Conceptualization, Methodology, Project Administration, Funding Acquisition. **Zhuo Zhou:** Conceptualization, Methodology, Project Administration, Writing - Original Draft, Funding Acquisition. **Li Guo:** Supervision, Writing - Reviewing & Editing. **Jianwei Wang:** Conceptualization, Project Administration, Funding Acquisition.

References

[1] WHO, WHO COVID-19 Dashboard. https://covid19.who.int, 2022 (accessed 29 April 2022).
[2] K.T. Choy, A.Y. Wong, P. Kaewpreedee, S.F. Sia, D. Chen, K.P.Y. Hui, D.K.W. Chu, M.C.W. Chan, P.P. Cheung, X. Huang, M. Peiris, H.L. Yen, Remdesivir, lopinavir, emetine, and homoharringtonine inhibit SARS-CoV-2 replication *in vitro*, Antiviral Res. 178 (2020), 104786. https://doi.org/10.1016/j.antiviral.2020.104786.
[3] B.M. Tomazini, I.S. Maia, A.B. Cavalcanti, O. Berwanger, R.G. Rosa, C.C.F. Fernandes, D.C. Morais, S. Zung, F.R. Machado, L.C.P. Azevedo, et al, Effect of dexamethasone on days alive and ventilator-free in patients with moderate or severe acute respiratory distress syndrome and COVID-19: the CoDEX randomized clinical trial, JAMA 324 (13) (2020) 1307–1316, https://doi.org/10.1001/jama.2020.17021.
[4] Y. Wang, D. Zhang, G. Du, R. Du, J. Zhao, T. Jaki, F.G. Hayden, P.W. Horby, B. Cao, C. Wang, et al, Remdesivir in adults with severe COVID-19: a randomised, double-blind, placebo-controlled, multicentre trial, Lancet 395 (10236) (2020) 1569–1578, https://doi.org/10.1016/s0140-6736(20)31022-9.
[5] L.L. Ren, Y.M. Wang, Z.Q. Wu, Z.C. Xiang, L. Guo, Z.H. Qian, C. Qin, Q. Jin, B. Cao, J.W. Wang, et al, Identification of a novel coronavirus causing severe pneumonia in human: a descriptive study, Chin. Med. J. (Engl) 133 (9) (2020) 1015–1024, https://doi.org/10.1097/CM9.0000000000000722.
[6] X. Yao, F. Ye, M. Zhang, C. Cui, B. Huang, X. Liu, R. Lu, H. Li, W. Tan, D. Liu, et al, *In vitro* antiviral activity and projection of optimized dosing design of hydroxychloroquine for the treatment of severe acute respiratory syndrome coronavirus 2 (SARS-CoV-2), Clin. Infect. Dis. 71 (15) (2020) 732–739, https://doi.org/10.1093/cid/ciaa237.
[7] A. Rismanbaf, S. Zarei, Liver and kidney injuries in COVID-19 and their effects on drug therapy; a letter to editor, Arch. Acad. Emerg. Med. 8 (1) (2020), e17.
[8] C. Doyno, D.M. Sobieraj, W.L. Baker, Toxicity of chloroquine and hydroxychloroquine following therapeutic use or overdose, Clin. Toxicol. (Phila) 59 (1) (2021) 12–23, https://doi.org/10.1080/15563650.2020.1817479.
[9] U.S. Food and Drug Administration, Coronavirus (COVID-19) update: FDA authorizes first oral antiviral for treatment of COVID-19. https://www.fda.gov/news-events/press-announcements/coronavirus-covid-19-update-fda-authorizes-first-oral-antiviral-treatment-covid-19, 2021 (accessed 22 December 2021).
[10] R. Singh, A. Gautam, S. Chandel, V. Sharma, A. Ghosh, D. Dey, S. Roy, V. Ravichandiran, D. Ghosh, Computational screening of FDA approved drugs of fungal origin that may interfere with SARS-CoV-2 spike protein activation, viral RNA replication, and post-translational modification: a multiple target approach, In Silico Pharmacol. 9 (1) (2021) 27, https://doi.org/10.1007/s40203-021-00089-8.
[11] W. Yin, C. Mao, X. Luan, D.D. Shen, Q. Shen, Y. Jiang, Y. Xu, S. Zhang, Y. Zhang, H. E. Xu, et al, Structural basis for inhibition of the RNA-dependent RNA polymerase from SARS-CoV-2 by remdesivir, Science 368 (6498) (2020) 1499–1504, https://doi.org/10.1126/science.abc1560.
[12] A.A. Elfiky, Ribavirin, Remdesivir, Sofosbuvir, Galidesivir, and Tenofovir against SARS-CoV-2 RNA dependent RNA polymerase (RdRp): a molecular docking study, Life Sci. 253 (2020), 117592. https://doi.org/10.1016/j.lfs.2020.117592.
[13] L. Fu, F. Ye, Y. Feng, F. Yu, Q. Wang, H. Song, X. Li, W. Tan, J. Qi, G.F. Gao, et al, Both Boceprevir and GC376 efficaciously inhibit SARS-CoV-2 by targeting its main protease, Nat. Commun. 11 (1) (2020) 4417, https://doi.org/10.1038/s41467-020-18233-x.
[14] Y. Zhao, X. Du, Y. Duan, X. Pan, Y. Sun, G. Xiao, L. Sun, L. Zhang, Z. Rao, H. Yang, et al, High-throughput screening identifies established drugs as SARS-CoV-2 PLpro inhibitors, Protein Cell. 12 (11) (2021) 877–888, https://doi.org/10.1007/s13238-021-00836-9.
[15] X. Xiao, C. Wang, D. Chang, Y. Wang, X. Dong, T. Jiao, Z. Zhao, L. Ren, C.S. Dela Cruz, L. Sharma, X. Lei, J. Wang, Identification of potent and safe antiviral therapeutic candidates against SARS-CoV-2, Front. Immunol. 11 (2020), 586572. https://doi.org/10.3389/fimmu.2020.586572.
[16] S. Boisson-Dupuis, X.F. Kong, S. Okada, S. Cypowyj, A. Puel, L. Abel, J.L. Casanova, Inborn errors of human STAT1: allelic heterogeneity governs the diversity of immunological and infectious phenotypes, Curr. Opin. Immunol. 24 (4) (2012) 364–378, https://doi.org/10.1016/j.coi.2012.04.011.
[17] Y. Han, X. Duan, L. Yang, B.E. Nilsson-Payant, P. Wang, F.C. Pan, T. Evans, H.J. Chen, R.E. Schwartz, S. Chen, et al, Identification of SARS-CoV-2 inhibitors using lung and colonic organoids, Nature 589 (7841) (2021) 270–275, https://doi.org/10.1038/s41586-020-2901-9.
[18] D.S. Baldwin, L. Chrones, I. Florea, R. Nielsen, G.G. Nomikos, W. Palo, E. Reines, The safety and tolerability of vortioxetine: analysis of data from randomized placebo-controlled trials and open-label extension studies, J. Psychopharmacol. 30 (3) (2016) 242–252, https://doi.org/10.1177/0269881116628440.
[19] H.L. Xiong, J.L. Cao, C.G. Shen, J. Ma, X.Y. Qiao, T.S. Shi, S.X. Ge, H.M. Ye, J. Zhang, Q. Yuan, T.Y. Zhang, N.S. Xia, Several FDA-approved drugs effectively inhibit SARS-CoV-2 infection *in vitro*, Front. Pharmacol. 11 (2020), 609592. https://doi.org/10.3389/fphar.2020.609592.
[20] M. Gopal, N. Padayatchi, J.Z. Metcalfe, M.R. O'Donnell, Systematic review of clofazimine for the treatment of drug-resistant tuberculosis, Int. J. Tuberc. Lung. Dis. 17 (8) (2013) 1001–1007, https://doi.org/10.5588/ijtld.12.0144.
[21] R. Sangana, H. Gu, D.Y. Chun, H.J. Einolf, Evaluation of clinical drug interaction potential of clofazimine using static and dynamic modeling approaches, Drug Metab Dispos. 46 (1) (2018) 26–32, https://doi.org/10.1124/dmd.117.077834.
[22] X. Zhang, Y. Shi, Z. Guo, X. Zhao, J. Wu, S. Cao, Y. Liu, Y. Li, W. Huang, Y. Wang, Q. Liu, Y. Li, D. Song, Clofazimine derivatives as potent broad-spectrum antiviral agents with dual-target mechanism, Eur. J. Med. Chem. 234 (2022), 114209. https://doi.org/10.1016/j.ejmech.2022.114209.
[23] S. Yuan, X. Yin, X. Meng, J.F. Chan, Z.W. Ye, L. Riva, D.Y. Jin, R. Sun, S.K. Chanda, K.Y. Yuen, et al, Clofazimine broadly inhibits coronaviruses including SARS-CoV-2, Nature 593 (7859) (2021) 418–423, https://doi.org/10.1038/s41586-021-03431-4.
[24] A. Carpinteiro, M.J. Edwards, M. Hoffmann, G. Kochs, B. Gripp, S. Weigang, K.A. Becker, S.A. Ahmad, K. Fassbender, E. Gulbins, et al, Pharmacological inhibition of acid sphingomyelinase prevents uptake of SARS-CoV-2 by epithelial cells, Cell. Rep. Med. 1 (8) (2020), 100142. https://doi.org/10.1016/j.xcrm.2020.100142.
[25] H. Peng, C. Ding, L. Jiang, W. Tang, Y. Liu, L. Zhao, Z. Yi, H. Ren, C. Li, Y. He, X. Zheng, H. Tang, Z. Chen, Z. Qi, P. Zhao, Discovery of potential anti-SARS-CoV-2 drugs based on large-scale screening *in vitro* and effect evaluation *in vivo*, Sci. China. Life. Sci. (2021) 1–17, https://doi.org/10.1007/s11427-021-2031-7.
[26] NIDDK, LiverTox: Clinical and research information on drug-induced liver injury, National Institute of Diabetes and Digestive and Kidney Diseases, Bethesda (MD), 2012.
[27] M. Otręba, L. Kośmider, A. Rzepecka-Stojko, Antiviral activity of chlorpromazine, fluphenazine, perphenazine, prochlorperazine, and thioridazine towards RNA-viruses. A review, Eur. J. Pharmacol. 887 (2020), 173553. https://doi.org/10.1016/j.ejphar.2020.173553.
[28] R.I. MacDonald, Trifluoperazine inhibits Sendai virus-induced hemolysis, Biochim. Biophys. Acta 856 (2) (1986) 337–347, https://doi.org/10.1016/0005-2736(86)90044-1.
[29] T. Zavorotinskaya, Z. Qian, J. Franks, L.M. Albritton, A point mutation in the binding subunit of a retroviral envelope protein arrests virus entry at hemifusion, J. Virol. 78 (1) (2004) 473–481, https://doi.org/10.1128/jvi.78.1.473-481.2004.